

Field-dependence of magnon decay in yttrium iron garnet thin films

A. L. Chernyshev¹

¹*Department of Physics, University of California, Irvine, California 92697, USA*

(Dated: November 8, 2018)

We discuss threshold field-dependence of the decay rate of the uniform magnon mode in yttrium iron garnet (YIG) thin films. We demonstrate that decays must cease to exist in YIG films of thickness less than $1\ \mu\text{m}$, the lengthscale defined by the exchange length. We show that due to the symmetry of the three-magnon coupling the decay rate is linear in $\Delta H = (H_c - H)$ in the vicinity of the threshold field H_c instead of the step-like $\Gamma_{\mathbf{k}=0} \propto \Theta(\Delta H)$ expected from the two-dimensional character of magnon excitations in such films. For thicker films, the decay rate should exhibit multiple steps due to thresholds for decays into a sequence of the two-dimensional magnon bands. For yet thicker films, such thresholds merge and crossover to the three-dimensional single-mode behavior: $\Gamma_{\mathbf{k}=0} \propto |\Delta H|^{3/2}$.

PACS numbers: 75.10.Jm, 75.40.Gb, 75.30.Ds

Introduction.—Extensive experimental and theoretical research on the ferromagnetic insulator, yttrium iron garnet $[\text{Y}_3\text{Fe}_2(\text{FeO}_4)_3]$ or YIG was started more than half a century ago has benefited from this material's exceptional purity, high Curie temperature, and relative simplicity of the low-energy magnon spectrum.¹ Recent discovery of the Bose-Einstein condensation of the highly occupied magnon states created by microwave pumping in YIG thin films has attracted substantial interest.² Recently, threshold effects due to the so-called three-magnon splitting have been reported in a quasi-two-dimensional (2D) thin films of YIG under microwave pumping and as a function of external field.³ In this, as well as in the other recent works,⁴ control over the spin current enhancement in layered metal-ferromagnet structures by the three-magnon processes is sought. This calls for a deeper theoretical insight into the decay dynamics of such structures. Fundamentally, given its outstanding properties,¹ YIG may offer a fertile playground in the studies of threshold phenomena, because the decay conditions in it can be varied continuously by both film thickness and external magnetic field.

Decays.—In this work, we discuss the decay rate of the uniform mode ($\mathbf{k}=0$ magnon) in an insulating ferromagnetic thin film as a function of external magnetic field and film thickness. In particular, using magnon dispersion in the lowest-mode approximation, we outline the ranges of the field and film thickness that favor decays in YIG. Specifically, we show that kinematic conditions for three-magnon decays cannot be met for the YIG films of thickness $d_{\text{min}} \approx 1\ \mu\text{m}$ or less and for the fields $H_c^{\text{max}} \approx 600\ \text{Oe}$ or higher. The upper limit on the external field is defined solely by the magnetization of a ferromagnet, in agreement with Ref. 3. Less obvious is the existence of the limit on the film thickness, which is fixed by another fundamental characteristics of a ferromagnet: its exchange length. The physical reason for that limit is the decreasing role of the long-range dipolar interactions with the decrease of the film thickness. The presence of such a limit must be important for the control of relaxation and transfer of the spin current in layered structures, which

rely on the three-magnon processes in YIG.⁴

We find that the threshold field-dependence of the decay rate for the $\mathbf{k}=0$ magnon near the threshold field H_c is $\Gamma_{\mathbf{k}=0} \propto |\Delta H| \cdot \Theta(\Delta H)$, where $\Delta H = (H_c - H)$, because the three-magnon interaction vanishes along the direction of the film magnetization, which is also precisely the \mathbf{k} -direction where magnon band minima are located. This leads to a reduction of the phase space for decays and results in a vanishing decay rate near the threshold, contrary the naïve expectation of the step-like increase of $\Gamma_{\mathbf{k}=0} \propto \Theta(\Delta H)$, when the symmetry of the three-magnon interaction is ignored.⁵ We have supported our consideration by explicit calculations of both $T=0$ and $T=300\text{K}$ relaxation rate dependencies on the field for several representative YIG film thicknesses.

The finite-size quantization in the film thickness direction leads to the formation of multiple magnon bands.⁶ We argue that the field-dependence for the decay rate should exhibit multiple steps linear in $|H_{c_i} - H|$, corresponding to the H_{c_i} thresholds for decays into a sequence of magnon bands. For thick films, these multiple thresholds should merge in a continuum, and the decay rate will crossover to a three-dimensional (3D) single-band behavior: $\Gamma_{\mathbf{k}=0} \propto |\Delta H|^{3/2}$. These results should be helpful in finding an optimal set of parameters for spin-current enhancement.³

Dispersion, density of states.—Despite its fairly complicated crystal structure, at low energies YIG can be described with great success as an effective large-spin Heisenberg ferromagnet on a cubic lattice with nearest-neighbor exchange, long-range dipolar interactions, and negligible spin anisotropy.^{1,7} Thus, at long wavelength, magnon energy in YIG is determined by a competition between three couplings: exchange, dipolar, and Zeeman. For a ferromagnetic crystal of the film geometry and external field directed in-plane where it co-aligns with the magnetization direction, as is done most commonly in experiments, the lowest-mode approximation for the

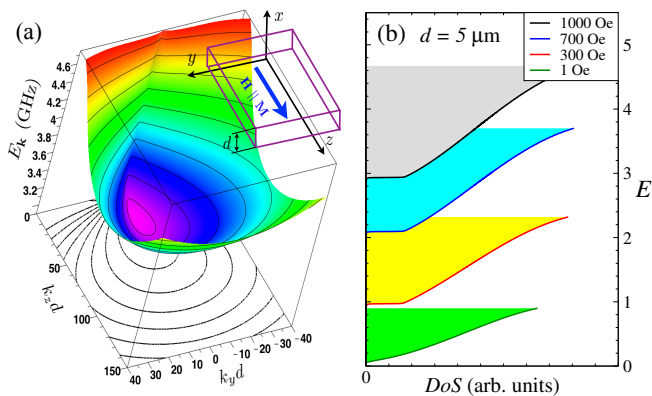


FIG. 1. (Color online) (a) 2D plot of magnon dispersion in YIG in the lowest-mode approximation, Eq. (1), for $H = 1000$ Oe, $d = 5 \mu\text{m}$, and in $k_z > 0$ sector. Inset: axes conventions relative to the film and the field/magnetization direction. (b) 2D magnon density of states (DoS) for several representative field values, E is in GHz.

magnon energy yields:^{5,6,8,9}

$$E_{\mathbf{k}} = \sqrt{(h + \rho\mathbf{k}^2 + \tilde{\Delta}_{\mathbf{k}} \sin^2 \theta_{\mathbf{k}})(h + \rho\mathbf{k}^2 + \Delta_{\mathbf{k}})}, \quad (1)$$

where $\Delta_{\mathbf{k}} = f_{\mathbf{k}}\Delta$ and $\tilde{\Delta}_{\mathbf{k}} = (1 - f_{\mathbf{k}})\Delta$ and $h = \mu H$, $\rho = JSa^2$, and $\Delta = 4\pi\mu M$ are the energy scale parametrizations of the external field, exchange, and dipolar interactions, respectively. The form factor $f_{\mathbf{k}} = (1 - e^{-|\mathbf{k}|d})/|\mathbf{k}|d$ is from the dipolar sums in the direction of the film thickness $d \gg a$, and $\theta_{\mathbf{k}}$ is the angle between the ferromagnet's magnetization (directed in-plane, z axis) and magnon's in-plane 2D wave vector \mathbf{k} , see Fig. 1(a). We use $\mu = g\mu_B$ where $g = 2$ is an effective g factor and μ_B is the Bohr magneton. In this work we adhere to the notations and units of Ref. 6, which has provided a detailed microscopic spin-wave theory of YIG in $1/S$ approximation, and we use experimental parameters for YIG, magnetization $4\pi M = 1750$ G, exchange stiffness $\rho/\mu = 5.17 \cdot 10^{-13}$ Oe m^2 , and lattice constant $a = 12.376$ Å. In Fig. 1(a), the magnon dispersion from Eq. (1) for a representative field $H = 1000$ Oe and film thickness $d = 5 \mu\text{m}$ is shown.

It should be noted that the dipolar interactions are responsible for the nontrivial structure of magnon band with the minima at finite wave vectors, which allow the decay conditions to occur. Although approximate, Eq. (1) provides a close quantitative description of the lowest 2D magnon energy band,⁶ quantized due to finite film thickness d in the x direction [Fig. 1(a), inset]. At small \mathbf{k} , dipolar interactions dominate over the exchange and result in a steep decrease from the energy of the uniform mode, $E_0 = \sqrt{h(h + \Delta)}$, for \mathbf{k} 's along the magnetization direction. At larger \mathbf{k} , exchange energy dominates, giving $E_{\mathbf{k}} \approx h + \rho\mathbf{k}^2$; while at intermediate \mathbf{k} , competition between exchange and dipolar terms results in peculiarly shaped minima at $\pm\mathbf{k}_m = (0, \pm k_m)$, see Fig. 1(a).

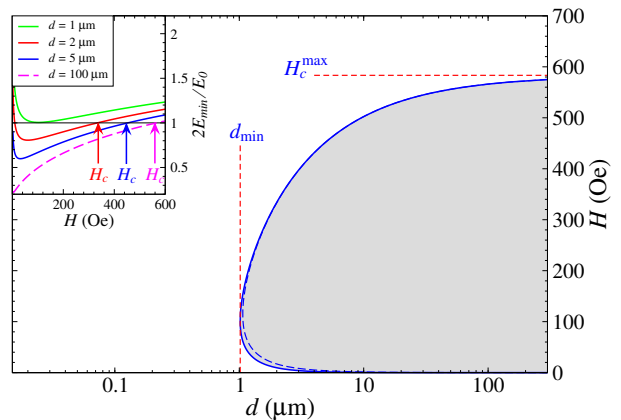


FIG. 2. (Color online) d - H decay diagram for YIG, shaded area is where decays are allowed. Solid (dashed) boundary is the numerical (analytical) solution for the threshold boundary, see text. H_{max} and d_{min} are shown. Inset: $2E_{\text{min}}/E_0$ vs H for several d 's, upper threshold fields are indicated.

The 2D density of magnon states from Eq. (1) is shown in Fig. 1(b) for several representative field values. Predictably, 2D DoS exhibits a step-like increase at the band minimum, which is followed by an unusual, almost linear increase, reminiscent of the similar behavior for the relativistic dispersion. The latter is due to a nonparabolicity of the long-wavelength magnon dispersion, see Fig. 1(a).

“Decay diagram”.—For the decays to take place the kinematic conditions must be fulfilled. For the two-magnon decay (three-magnon splitting) of the uniform mode, the condition to be satisfied is simply $E_0 = 2E_{\mathbf{q}}$. With the microscopic parameters, such as exchange stiffness and magnetization, fixed, some other parameters can be varied to allow or to forbid decays altogether. As is clear from Eq. (1), the external field increases the energies of both the uniform mode and the minimum, making decays kinematically impossible at some higher field value.³ Another parameter is the film thickness d , which enters Eq. (1) through the form factor $f_{\mathbf{k}}$. While the manner in which d influences decays is not *a priori* clear, both trends, vs field and vs thickness, can be examined numerically. Such an examination is exemplified in Fig. 2, which shows $2E_{\text{min}}/E_0$ vs field for several film thicknesses. Clearly, when the plotted quantity is < 1 , decays are allowed, and the crossing of 1 corresponds to a threshold field for decays.

Our Fig. 2 gives the complete d - H “decay diagram” for YIG with the shaded area showing the parameter space where decays are allowed. Two key results are clear in Fig. 2: (i) the upper threshold field does not exceed some $H_{\text{c}}^{\text{max}}$ even for large values of d , and (ii) there exists a lower limit on the film thickness d_{min} , below which the decays of the uniform mode may not occur at all. The solid boundary is the numerical solution of Eq. (1) for the energy minimum and the decay conditions. The dashed line is an approximate analytical solution, which turns out to be very precise. The latter also gives us a deeper

insight into the nature of H_c^{\max} and d_{\min} discussed next.

Large- $|\mathbf{k}_m|d$ approximation—At large enough d the wavevector of the magnon energy minimum satisfies $|\mathbf{k}_m|d \gg 1$. Then the formfactor $f_{\mathbf{k}_m} \approx 1/|\mathbf{k}_m|d$ is small, reflecting the reduced role of dipolar interactions in the energy of the \mathbf{k}_m -magnon. One can then show¹⁰ that both the exchange and the dipolar energies for the \mathbf{k}_m -magnon scale as $\propto d^{-2/3}$ and thus are $\ll h$ for any reasonable field. This implies that the energy of the magnon band minimum is $E_{\min} \approx h$, expected for the uniform mode in the absence of dipolar interactions. Then, the decay threshold equation, $2E_{\min} = E_0$, trivially gives $h_c = \Delta/3$, relating saturated value of the decay threshold field to the material's magnetization: $H_c^{\max} = 4\pi M/3$ ($= 583$ Oe for YIG in Fig. 2(b)), see also Ref. 3.

The physical question is: what parameter of the ferromagnet defines d_{\min} ? One can extend the large- $|\mathbf{k}_m|d$ approach and find¹⁰ that the energies of the dipolar and exchange interactions must be related by $|\mathbf{k}_m|d = (\Delta d^2/4\rho)^{1/3}$. With this, the decay threshold condition $2E_{\min} = E_0$ leads to an algebraic equation in H_c vs d , which can be resolved in a compact form.¹⁰ It is plotted as a dashed line in Fig. 2(b), which coincides almost exactly with the decay boundary obtained from Eq. (1) numerically. From the same equation we find the minimal thickness to be $d_{\min} \approx C\sqrt{\rho/\Delta}$, explicitly related to the exchange length of the ferromagnet, $\ell_{ex} = \sqrt{\rho/\Delta}$, albeit with a large numerical coefficient $C \approx 62.04$.¹⁰ Using parameters for YIG, the exchange length is $\ell_{ex} \approx 13.9a$ and the minimum thickness $d_{\min} = 1.067 \mu\text{m}$, remarkably close to the numerical result $d_{\min} = 1.017 \mu\text{m}$.

The physical reason for the very existence of d_{\min} is the decreasing role of long-range dipolar interactions in the magnon's energy with the decrease of film thickness, as the relation of d_{\min} to exchange length implies. The fact that the decay boundary in d exceeds the exchange length by a large numerical factor is due to the rather stringent requirements of the decay conditions. We emphasize that the provided d - H diagram should apply equally to the other thin-film ferromagnets.

Decay rate.—Transitions that involve changing the number of magnons, such as decays, recombination, or coalescence, originate from the dipolar interactions that couple longitudinal and transverse spin components and therefore do not conserve magnetic^{1,7} as well as mechanical angular momentum.³ Microscopically, dipolar interactions result in anharmonic couplings of magnons, which, for the decay processes of the $\mathbf{k} = 0$ uniform mode into two magnons at \mathbf{q} and $-\mathbf{q}$, can be written as

$$\mathcal{H}^{(3)} = \frac{1}{2} \sum_{\mathbf{q}} V_{0;\mathbf{q},-\mathbf{q}}^{(3)} \left(a_{\mathbf{q}}^\dagger a_{-\mathbf{q}}^\dagger a_0 + \text{H.c.} \right). \quad (2)$$

The three-magnon coupling in Eq. (2) has an angular dependence: $V_{0;\mathbf{q},-\mathbf{q}}^{(3)} = V_0 \sin 2\theta_{\mathbf{q}}$, with $V_0 = \Delta/\sqrt{2S}$.^{1,11,12} This angular dependence is essential since it reflects the symmetry of dipolar coupling of the transverse, S^x (S^y), and longitudinal, S^z , spin components: $V^{xz} \propto xz/r^3$

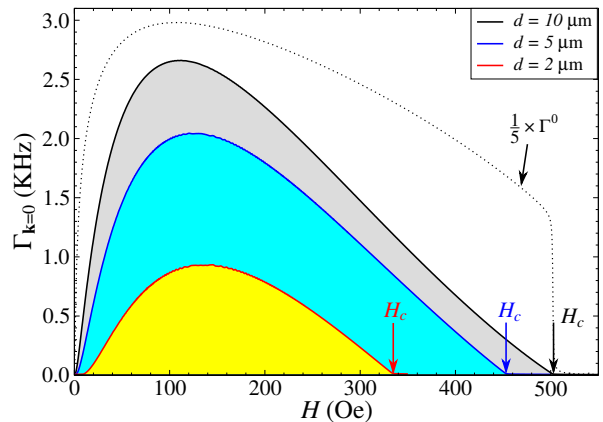


FIG. 3. (Color online) The $T = 0$ decay rate $\Gamma_{\mathbf{k}=0}$ vs H for $d = 2, 5,$ and $10 \mu\text{m}$. Dotted line is $\frac{1}{5}\Gamma_{\mathbf{k}=0}$ for $d = 10 \mu\text{m}$ with the angular-dependence of the three-magnon coupling omitted, $V_{0;\mathbf{q},-\mathbf{q}}^{(3)} \Rightarrow V_0$.

($V^{yz} \propto yz/r^3$). In particular, it is natural for this coupling to vanish for the spin-wave propagating with the momentum \mathbf{q} along the direction of magnetization \mathbf{M} [z axis, Fig. 1(a)].¹¹ We would like to point out that it is also precisely the direction along which the minima of the magnon band are located.¹³ Therefore, the amplitude of the decay of $\mathbf{k} = 0$ magnon into two magnons at the band minima \mathbf{q}_m and $-\mathbf{q}_m$ is zero. This will lead to a rather spectacular violation of the naïve expectation: while kinematic conditions for the decay of $\mathbf{k} = 0$ magnon into $\pm\mathbf{q}_m$ are just met at H_c , the corresponding decay amplitude is vanishing. Thus, the decay rate must increase gradually from the threshold, not in a jump-like fashion as in the DoS, Fig. 1(b).

At $T = 0$ only spontaneous magnon decays are allowed.¹⁴ The three-magnon recombination processes have to obey the same kinematic constraints as the decay, having therefore the same threshold conditions. The three-magnon coalescence processes involving the $\mathbf{k} = 0$ mode correspond to the “vertical” transitions, which are forbidden either kinematically as in the single mode case or by the quantum number of the interband transition in the multi-band situation. The four-magnon scattering amplitude from the exchange interaction vanishes identically for the uniform mode, while the remaining four-magnon interactions from the dipole-dipole interaction together with impurity scattering should be providing a background with weak H and T dependence, distinct from the threshold behavior discussed here.

With this in mind, using the kinetic approach,^{1,7} which takes into account the balance between decay and recombination processes in the relaxation time approximation, the decay rate¹⁵ of the uniform mode is

$$\Gamma_{\mathbf{k}=0} = \pi \sum_{\mathbf{q}} |V_{0;\mathbf{q},-\mathbf{q}}^{(3)}|^2 [2n_{\mathbf{q}} + 1] \delta(E_0 - 2E_{\mathbf{q}}) \quad (3)$$

where $n_{\mathbf{q}} = [e^{\hbar E_{\mathbf{q}}/k_b T} - 1]^{-1}$ is the Bose occupation factor. It is clear from Eq. (3) that while the magnitude of

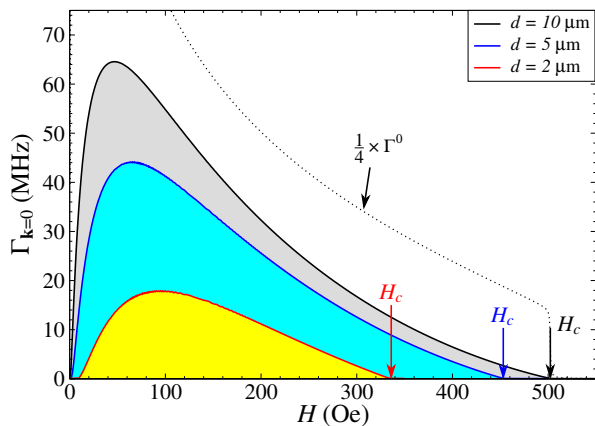


FIG. 4. (Color online) Same as in Fig. 3, but for $T = 300$ K.

the decay rate at finite T can be substantially modified from the $T = 0$ result by the Bose-occupation factors, the qualitative threshold behavior must remain the same.

One can investigate the threshold behavior of Eq. (3) analytically and obtain $\Gamma_{\mathbf{k}=0} \propto |E_0 - 2E_{\min}|$ for $H \rightarrow H_c$.¹⁰ Given the proportionality between $(E_0 - 2E_{\min})$ and $\Delta H = (H_c - H)$ demonstrated in Fig. 2, this yields *linear* dependence of the decay rate on the field relative to the threshold: $\Gamma_{\mathbf{k}=0} \propto |\Delta H| \cdot \Theta(\Delta H)$, see Figs. 3 and 4. Once again, this is the consequence of an effective suppression of the phase space for decays due to the discussed angular dependence of the three-magnon coupling.

In Figs. 3 and 4 we show $\Gamma_{\mathbf{k}=0}$ for three different film thicknesses and for $T = 0$ and $T = 300$ K, respectively. While the overall scale in the two figures is in a completely different frequency range,¹⁰ the shapes of Γ vs H are qualitatively very similar, especially concerning their threshold behavior vs field, in agreement with the above analysis. The relative difference between the curves for different d 's reflects the smaller phase space for decays in thinner films. In the same Figs. 3 and 4 we demonstrate a dramatic contrast with the results of Eq. (3) if the angular dependence of the three-magnon coupling in Eq. (2) is neglected, $V_{0;\mathbf{q},-\mathbf{q}}^{(3)} \Rightarrow V_0$. The latter results exhibit jumps at H_c 's and a linear increase after that, similar to the 2D magnon DoS in Fig. 1(b). One should also note that the overall decay rate is also markedly overestimated if the angular dependence of the three-magnon interaction

is ignored.

In thicker films, the decay rate will be further modified by the multiple magnon bands that occur due to finite-size quantization in the film thickness direction.⁶ It will exhibit a sequence of steps linear in $|H_{c_i} - H|$, where H_{c_i} is the threshold field for decay into an i th band, increasing the decay rate every time the corresponding kinematic conditions are met. Strictly speaking, the angle $\theta_{\mathbf{q}}$ in $V_{0;\mathbf{q},-\mathbf{q}}^{(3)}$ is between the 3D \mathbf{q} vector and magnetization vector \mathbf{M} . In the quasi-2D geometry with the levels quantized in the x directions, q_x has discrete values and the minimal value of $\theta_{\mathbf{q}_i}^{\min} \approx q_{x,i}^{\min}/|\mathbf{q}|$ is zero only for the lowest magnon band. Thus, the thresholds in H_{c_i} 's will have some small step-like behavior. However, this effect must be negligibly smaller compared to the steps in Figs. 3 and 4 when the angular dependence in $V^{(3)}$ is ignored altogether. Extending our analysis to the limit of thicker films where multiple bands merge into a single 3D band, using Eq. (3) we obtain¹⁰ that the decay rate near the threshold field will crossover to $\Gamma_{\mathbf{k}=0} \propto |\Delta H|^{3/2}$.

Conclusions.— In this work, we have discussed the field-dependence of the decay rate of the uniform magnon mode in YIG thin films and the effects of film thickness in it. As a result of our analysis, we have established that the two key characteristics of a ferromagnet, its magnetization and exchange length, define the extent of the $d-H$ parameter range that favors decays in thin film geometry. Our calculations of the decay rate should provide an important guidance for the experimentalists in designing the optimal conditions for the control of spin current and its relaxation in thin films. A particularly intriguing suggestion to pursue is to study the properties of a thin film with varying thickness, which may permit decays and, as a consequence, the spin current enhancement in one part of the film and forbid it in the other.

Acknowledgments.—I am deeply indebted to Doug Mills for introducing me to this problem, for many illuminating discussions and constant encouragement. I thank Ilya Krivorotov for numerous enlightening conversations, his genuine interest and support, as well as generosity with his time spent on educating me in this field. I also acknowledge useful conversation with Andreas Kreisel. This work was supported by the U.S. DoE under grant DE-FG02-04ER46174.

¹ V. Cherepanov, I. Kolokolov, and V. L'vov, Phys. Rep. **229**, 81 (1993).

² S. O. Demokritov, V. E. Demidov, O. Dzyapko, G. A. Melkov, A. A. Serga, B. Hillebrands, and A. N. Slavin, Nature **443**, 430 (2006); V. E. Demidov, O. Dzyapko, S. O. Demokritov, G. A. Melkov, and A. N. Slavin, Phys. Rev. Lett. **99**, 037205 (2007); **100**, 047205 (2008).

³ H. Kurebayashi, O. Dzyapko, V. E. Demidov, D. Fang, A. J. Ferguson, and S. O. Demokritov, Nature Mater. **10**, 660

(2011).

⁴ K. Ando and E. Saitoh, Phys. Rev. Lett. **109**, 026602 (2012); Z. Wang, Y. Sun, M. Wu, V. Tiberkevich, and A. Slavin, Phys. Rev. Lett. **107**, 146602 (2011); H. Schultheiss, X. Janssens, M. van Kampen, F. Ciubotaru, S. J. Hermsdoerfer, B. Obry, A. Laraoui, A. A. Serga, L. Lagae, A. N. Slavin, B. Leven, and B. Hillebrands, Phys. Rev. Lett. **103**, 157202 (2009).

⁵ S. M. Rezende, Phys. Rev. B **79**, 174411 (2009).

- ⁶ A. Kreisel, F. Sauli, L. Bartosch, and P. Kopietz, *Eur. Phys. J. B* **71**, 59 (2009).
- ⁷ A. G. Gurevich and G. A. Melkov, *Magnetization Oscillations and Waves*, (CRC Press, Boca Raton, 1996).
- ⁸ I. S. Tupitsyn, P. C. E. Stamp, and A. L. Burin, *Phys. Rev. Lett.* **100**, 257202 (2008).
- ⁹ B. A. Kalinikos and A. N. Slavin, *J. Phys. C* **19**, 7013 (1986).
- ¹⁰ See supplemental material for details of the calculations of the $d-H$ decay boundary and of the decay rate threshold field-dependence.
- ¹¹ M. Sparks and C. Kittel, *Phys. Rev. Lett.* **4**, 232, 320 (1960).
- ¹² M. Sparks, R. Loudon, and C. Kittel, *Phys. Rev.* **122**, 791 (1961); E. Schlömann, *Phys. Rev.* **121**, 1312 (1961); B. Lemaire, H. Le Gall, and J. L. Dormann, *Solid State Commun.* **5**, 499 (1967); A. V. Syromyatnikov, *Phys. Rev. B* **82**, 024432 (2010).
- ¹³ J. Hick, F. Sauli, A. Kreisel, and P. Kopietz, *Eur. Phys. J. B* **78**, 429 (2010).
- ¹⁴ M. E. Zhitomirsky and A. L. Chernyshev, arXiv:1205.5278.
- ¹⁵ Our $\Gamma_{\mathbf{k}=0}$ corresponds to half-width at half-maximum, *i.e.*, $\Gamma_{\mathbf{k}=0} = \frac{1}{2}\tau_{\mathbf{k}=0}^{-1}$.

I. SUPPLEMENTAL MATERIAL

A. large- $|\mathbf{k}_m|d$ approximation

Assuming that for large enough d the magnon energy minimum satisfies $|\mathbf{k}_m|d \gg 1$, makes the formfactor $f_{\mathbf{k}} = (1 - e^{-|\mathbf{k}_m|d})/|\mathbf{k}_m|d \approx 1/|\mathbf{k}_m|d$ small and allows to simply $E_{\mathbf{k}}$ in Eq. (1) to an algebraic expression in reduced energy scales of the dipolar and exchange interactions, $\bar{\Delta} = \Delta/|\mathbf{k}_m|d$ and $\bar{\rho} = \rho/|\mathbf{k}_m|^2$:

$$E_{\mathbf{k}_m} = \sqrt{(h + \bar{\rho})(h + \bar{\rho} + \bar{\Delta})}, \quad (1)$$

where we also used the fact that the minimum is located along the z -axis, so $\theta_{\mathbf{k}_m} = 0$. The minimum condition $\partial E_{\mathbf{k}}/\partial \mathbf{k} = 0$ yields:

$$h + \bar{\rho} + \frac{\bar{\Delta}}{4} = h \cdot \frac{\bar{\Delta}}{4\bar{\rho}}, \quad (2)$$

which, in the limit of both reduced exchange and dipolar energy scales being small compared to the field, $\bar{\rho}, \bar{\Delta} \ll h$, yields a straightforward relation between the two:

$$\bar{\Delta} = 4\bar{\rho}. \quad (3)$$

This relation gives the field-independent answer for $|\mathbf{k}_m|d$:

$$|\mathbf{k}_m|d = \left(\frac{\Delta d^2}{4\rho}\right)^{1/3}, \quad (4)$$

which justifies the above approximation $\bar{\rho}, \bar{\Delta} \ll h$ for large enough d because:

$$\bar{\Delta} = 4\bar{\rho} = \left(\frac{4\rho\Delta^2}{d^2}\right)^{1/3}. \quad (5)$$

Having the dipolar and exchange scales related by Eq. (3), we can substitute it into Eq. (1) for E_{\min} and use it to solve the decay threshold condition $2E_{\min} = E_0$ with $E_0 = \sqrt{h(h + \Delta)}$. This leads to a quadratic equation in the threshold field $h_c (= \mu H_c)$ vs $\bar{\Delta}$ (which, in turn, is a function of d by Eq. (5)), that can be resolved in a compact form:

$$h_{c_{1,2}} = \left(\frac{\Delta}{6} - \bar{\Delta}\right) \pm \sqrt{\left(\frac{\Delta}{6} - \bar{\Delta}\right)^2 - \frac{5}{12}\bar{\Delta}^2}, \quad (6)$$

with two solutions being the upper and the lower threshold fields. They give the (approximate) threshold boundary in Fig. 2(b), shown by the dashed line. From the same solution one can find the ‘‘maximal’’ $\bar{\Delta}_m$ that corresponds to the lower boundary on $d = d_{\min}$ for which the solution of the threshold condition exists. This is also the point at which $h_{c_1} = h_{c_2}$ in Eq. (6) and the content of the square-root is zero, solving for which gives

$$\bar{\Delta}_m = \bar{\Delta}(d_{\min}) = \left(\frac{6 - \sqrt{15}}{21}\right) \Delta. \quad (7)$$

Using Eq. (5) we finally obtain:

$$d_{\min} = 2 \left(\frac{21}{6 - \sqrt{15}}\right)^{3/2} \sqrt{\frac{\rho}{\Delta}} \approx 62.04 \sqrt{\frac{\rho}{\Delta}}. \quad (8)$$

Although the following result can be trivially obtained from the solution for h_{c_1} in Eq. (6) taking the $d \rightarrow \infty$ limit ($\bar{\Delta} \rightarrow 0$), one can derive the large- d limit for $H_{c_1} \rightarrow H_c^{\max}$ via an observation that at $d \rightarrow \infty$ energy minimum in Eq. (1) is $E_{\min} \approx h$, as $\bar{\Delta}, \bar{\rho} \rightarrow 0$. This reduces the decay condition to a simple one:

$$2h_c = \sqrt{h_c(h_c + \Delta)}, \quad (9)$$

with two solutions: $h_{c_2} = 0$ and $h_{c_1} = \mu H_c^{\max} = \Delta/3$, thus relating the saturated magnetization of the material to the upper limit of the threshold field for decays.

B. threshold field-dependence of $\Gamma_{\mathbf{k}=0}$

Since we are interested in the threshold behavior, only spontaneous ($T = 0$) decay rate is considered. Near the threshold, decays are happening into the magnons in the vicinity of the magnon band minima $\pm \mathbf{q}_m = (0, \pm q_m)$. Expanding in $(\mathbf{q} - \mathbf{q}_m)$ near the minima gives:

$$\begin{aligned} \Gamma_{\mathbf{k}=0} &= \pi \sum_{\mathbf{q}} |V_{0;\mathbf{q},-\mathbf{q}}^{(3)}|^2 \delta(E_0 - 2E_{\mathbf{q}}) \\ &= \frac{V_0^2}{2\pi} \int_{-\pi}^{\pi} dq_y \int_0^{\pi} dq_z \sin^2 2\theta_{\mathbf{q}} \delta\left(\Delta E - \frac{\Delta \mathbf{q}^2}{m}\right), \end{aligned} \quad (10)$$

where $\Delta \mathbf{q} = (\mathbf{q} - \mathbf{q}_m)$, $\Delta E = (E_0 - 2E_{\min})$ and m is the effective magnon mass. Rewriting $\sin 2\theta_{\mathbf{q}}$ as $2q_y q_z / \mathbf{q}^2$ and shifting integration in q_z by q_m yields

$$\Gamma_{\mathbf{k}=0} = \frac{2V_0^2}{\pi |\mathbf{q}_m|^2} \int q_y^2 dq_y \int d\bar{q}_z \delta\left(\Delta E - \frac{\bar{\mathbf{q}}^2}{m}\right), \quad (11)$$

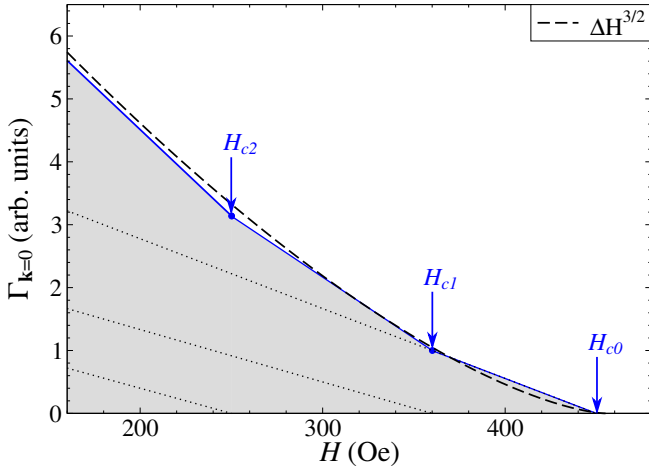


FIG. 5. (Color online) A sketch of $\Gamma_{\mathbf{k}=0}$ vs H for the case of multiple magnon bands. Dotted lines show linear in $|H_{c_i} - H|$ contributions of each band, solid line with the shading is the total effect, dashed line is the 3D limit $\propto \Delta H^{3/2}$.

where $\bar{q}_z = q_z - q_m$, $\bar{\mathbf{q}}^2 = \bar{q}_z^2 + q_y^2$, and in approximating $\mathbf{q}^2 \approx \mathbf{q}_m^2$ the smallness of \bar{q}_z 's and q_y 's in comparison

with $|\mathbf{q}_m|$ was used. It finally leads to:

$$\Gamma_{\mathbf{k}=0} = \frac{V_0^2 m^2}{|\mathbf{q}_m|^2} |E_0 - 2E_{\min}|. \quad (12)$$

Since $|E_0 - 2E_{\min}| \propto |H_c - H|$, this yields $\Gamma_{\mathbf{k}=0} \propto \Delta H$.

At finite $T \gg E_{\min}$, the decay rate near the threshold is

$$\Gamma_{\mathbf{k}=0} = \frac{2T^2}{E_{\min}^2} \frac{V_0^2 m^2}{|\mathbf{q}_m|^2} |E_0 - 2E_{\min}|. \quad (13)$$

For the 3D case, when the 2D bands merge into a continuum, the above consideration results in:

$$\Gamma_{\mathbf{k}=0}^{3D} \propto \frac{V_0^2}{|\mathbf{q}_m|^2} \int q_{\perp}^3 dq_{\perp} d\bar{q}_z \delta\left(\Delta E - \frac{\bar{\mathbf{q}}^2}{m}\right), \quad (14)$$

where $\bar{\mathbf{q}}^2 = \bar{q}_z^2 + q_{\perp}^2$ now and possible mass anisotropies, while neglected, are not going to change the result qualitatively:

$$\Gamma_{\mathbf{k}=0}^{3D} \propto \frac{V_0^2 m^2}{|\mathbf{q}_m|^2} |E_0 - 2E_{\min}|^{3/2}, \quad (15)$$

and thus, $\Gamma_{\mathbf{k}=0}^{3D} \propto \Delta H^{3/2}$.